Combination of methylated-DNA precipitation and methylation-sensitive restriction enzymes (COMPARE-MS) for the rapid, sensitive and quantitative detection of DNA methylation

Srinivasan Yegnasubramanian[1], Xiaohui Lin[1], Michael C. Haffner[1,2], Angelo M. DeMarzo[1] and William G. Nelson[1,*]

[1]Sidney Kimmel Comprehensive Cancer Center, The Johns Hopkins University School of Medicine, 1650 Orleans Street, CRB 116, Baltimore, MD 21231, USA and [2]Innsbruck Medical University, Christoph-Probst-Platz 1, Innrain 52, A-6020 Innsbruck, Austria

ABSTRACT

Hypermethylation of CpG island (CGI) sequences is a nearly universal somatic genome alteration in cancer. Rapid and sensitive detection of DNA hypermethylation would aid in cancer diagnosis and risk stratification. We present a novel technique, called COMPARE-MS, that can rapidly and quantitatively detect CGI hypermethylation with high sensitivity and specificity in hundreds of samples simultaneously. To quantitate CGI hypermethylation, COMPARE-MS uses real-time PCR of DNA that was first digested by methylation-sensitive restriction enzymes and then precipitated by methyl-binding domain polypeptides immobilized on a magnetic solid matrix. We show that COMPARE-MS could detect five genome equivalents of methylated CGIs in a 1000- to 10 000-fold excess of unmethylated DNA. COMPARE-MS was used to rapidly quantitate hypermethylation at multiple CGIs in >155 prostate tissues, including benign and malignant prostate specimens, and prostate cell lines. This analysis showed that *GSTP1*, *MDR1* and *PTGS2* CGI hypermethylation as determined by COMPARE-MS could differentiate between malignant and benign prostate with sensitivities >95% and specificities approaching 100%. This novel technology could significantly improve our ability to detect CGI hypermethylation.

INTRODUCTION

DNA methylation at the 5-position of cytosine in CpG dinucleotides is an important aspect of physiological processes including embryonic development, X chromosome inactivation, imprinting and transcriptional regulation (1–4). While CpG dinucleotides are generally methylated throughout the genome of normal somatic cells, CpG islands (CGIs), clusters of CpG dinucleotides in gene regulatory regions, are usually unmethylated (5). Aberrant hypermethylation of CGIs and subsequent transcriptional repression is one of the earliest and most common somatic genome alterations in multiple human cancers (6,7). Some cancers even seem to exhibit a so-called CpG island methylator phenotype (CIMP) (8). The rapid and sensitive detection of DNA hypermethylation, therefore, would not only enhance our understanding of how DNA methylation may contribute to carcinogenesis, but could aid in early cancer diagnosis and risk stratification (9,10).

Most of the current DNA methylation detection strategies use sodium bisulfite to deaminate cytosine to uracil while leaving 5-methylcytosine intact (11). Among these, methylation-specific PCR (MSP) (12) uses PCR primers targeting the bisulfite induced sequence changes to specifically amplify either methylated or unmethylated alleles. Quantitative variations of this technique, such as MethyLight (13), HeavyMethyl (14) and MethylQuant (15), employ methylation-specific oligonucleotides in conjunction with Taqman probes or SYBR Green based real-time PCR amplification to quantitate alleles with a specific pattern of methylation. These techniques are highly sensitive and specific for detection of DNA methylation. However, all of the bisulfite-based techniques are quite cumbersome, involving

time- and labor-intensive chemical treatments that damage DNA and limit throughput. Additionally, PCR primer design becomes difficult due to the reduction in genome complexity after bisulfite treatment, leading to an inability to interrogate the methylation pattern at some or all CpG dinucleotides in a genomic locus of interest.

Other DNA methylation detection assays use methylation-sensitive restriction enzymes to digest unmethylated DNA while leaving methylated DNA intact for detection by Southern blot analysis (16–19), PCR (20,21) or real-time PCR (22). The Southern blot strategy is not easily amenable to high-throughput analysis and requires copious amounts of high molecular weight DNA. Digestion followed by PCR is sensitive, but is limited to interrogating methylation only at the enzyme recognition sites and is plagued by a propensity for false-positives resulting from incomplete digestion.

Another strategy for *in vitro* methylation detection, first introduced in 1994 by Cross et al (23), uses column- or bead-immobilized recombinant methylated-CpG binding domain (MBD) proteins, particularly MECP2 (23–25) and MBD2 (26), to enrich for methylated DNA fragments for subsequent detection by Southern blot, PCR or microarray hybridization. The MBD proteins are thought to bind specifically to methylated chromosomal DNA in mammalian cells (27), facilitating transcriptional silencing (28,29) by recruitment of chromatin remodeling and transcriptional repression complexes (30,31). A recent version of this strategy, called MIRA (26), uses full-length MBD2 immobilized on magnetic beads to enrich for methylated DNA with subsequent detection of candidate methylated genes by PCR. Another assay, termed MeDIP (32), uses bead-immobilized anti-5-methylcytosine antibodies (α5mC-Abs), instead of MBD proteins, to enrich for methylated DNA. However, the use of each these techniques has been limited by one or more of the following: a requirement for relatively large amounts of input genomic DNA, a potential for false-positive results due to capture of unmethylated DNA, incompatibility with high-throughput platforms and lack of quantitative data.

In this study, we report the use of a novel technique, called COMPARE-MS, that combines the use of methylation-sensitive restriction enzymes with MBD assisted capture and enrichment of methylated DNA followed by quantitative PCR for sensitive, specific and rapid quantitation of hypermethylated CGI sequences. We show that these two strategies in combination complement each other, eliminating many of the problems associated with using either technique alone, while achieving sensitivities and specificities comparable with MSP, MethyLight and other bisulfite treatment-based PCR techniques. Additionally, COMPARE-MS was highly amenable to high-throughput, 96-well plate analysis, and was used to rapidly determine the quantitative hypermethylation pattern at multiple CGIs for 155 prostate tissue specimens, including malignant and benign tissues, and multiple prostate cell lines.

MATERIALS AND METHODS

Cell culture, tissue samples and DNA isolation

Genomic DNA from LNCaP, PC3, LAPC4, C42B and CWR22Rv1 prostate cancer cell lines, PrEC normal prostate cells, prostate benign tissues from 13 brain-dead transplant tissue donors with no evidence of prostate disease, primary prostate cancer tissues from 130 men undergoing radical prostatectomy and tumor-adjacent benign tissues from 12 of these 130 men, were obtained as described previously (33). DNA quantitation was carried out prior to restriction enzyme digestion and MBD2-MBD capture and was performed by UV absorbance on a standard spectrophotometer and verified by real-time PCR of the Beta-globin gene to ensure that DNA was of ample quality for reliable quantitative PCR amplification (22,34).

Cloning, expression and purification of MBD2-MBD polypeptides

To produce recombinant His$_6$-tagged MBD polypeptides from the human MBD2 (MBD2-MBD), *MBD2-MBD* cDNA sequence was amplified from clone MGC-45084 (American Type Culture Collection), using PCR primers 5′-GGATCCATGGAGAGCGGGAAGAGGATGGA and 5′-GAATTCCATCTTTCCAGTTCTGAAGT containing BamHI and EcoRI recognition sites. A modified pFastBac 1 baculovirus expression vector (Invitrogen), pFBC6H, was generated by inserting the sequence CGCGGCAGCCAT-CACCATCACCATCACTAA, which encodes a 6-histidine tag, into pFastBac 1 between the EcoRI and XbaI sites. The PCR amplified cDNA sequences were then introduced into pFBC6H after linearization with BamHI and EcoRI. The pFBC6H-*MBD2-MBD* expression constructs were used to transform DH10Bac™ *Escherichia coli* Competent Cells (Invitrogen) to form MBD expression bacmids via site-specific transposition. The expression bacmids were then transfected into Sf9 insect cells for production of recombinant MBD2-MBD polypeptide encoding baculovirus particles, which were used to infect additional Sf9 cells (1 MOI, 48 h) to generate recombinant MBD2-MBD proteins containing a C-Terminal 6x histidine tag. Recovery of recombinant 6-His-tagged MBD2-MBD polypeptides was accomplished by methods similar to those described previously (35). Briefly, the infected Sf9 cell pellets were resuspended in native binding buffer containing 50 mM NaPO$_4$, 0.5 M NaCl, 10 mM imidazole and 1× Complete EDTA-free Protease Inhibitor cocktail (Roche Diagnostics). Cells were lysed by two freeze-thaw cycles and the DNA was sheared by passing the sample through 20-gauge needles 4–6 times. The soluble fraction was mixed with pre-washed Ni-NTA Superflow resin (Qiagen) and incubated at 4°C for 2 h with rotation to allow maximum binding. The supernatant, designated as flow-through, was removed after centrifugation for 1 min at 1000 r.p.m. (IEC HN-SII Centrifuge). The resin was washed three times with 1× Native Wash Buffer containing 50 mM NaPO$_4$, 0.5 M NaCl, 35 mM imidazole and 1× Complete EDTA-free Protease Inhibitor cocktail. The recombinant proteins were then eluted from the resin with Native Elution Buffer (50 mM NaPO$_4$, 0.5 M NaCl, 250 mM imidazole and protease inhibitor cocktail). The eluates were subjected to buffer exchange using an Amicon Ultra-15 centrifugal filter device (5000 MWCO, Millipore). The recombinant proteins were stored in buffer containing 20 mM HEPES buffer, 0.1 M KCl, 0.2 mM EDTA, 0.5 mM DTT, 20% glycerol and 1× Complete EDTA-free Protease Inhibitor cocktail at −80°C
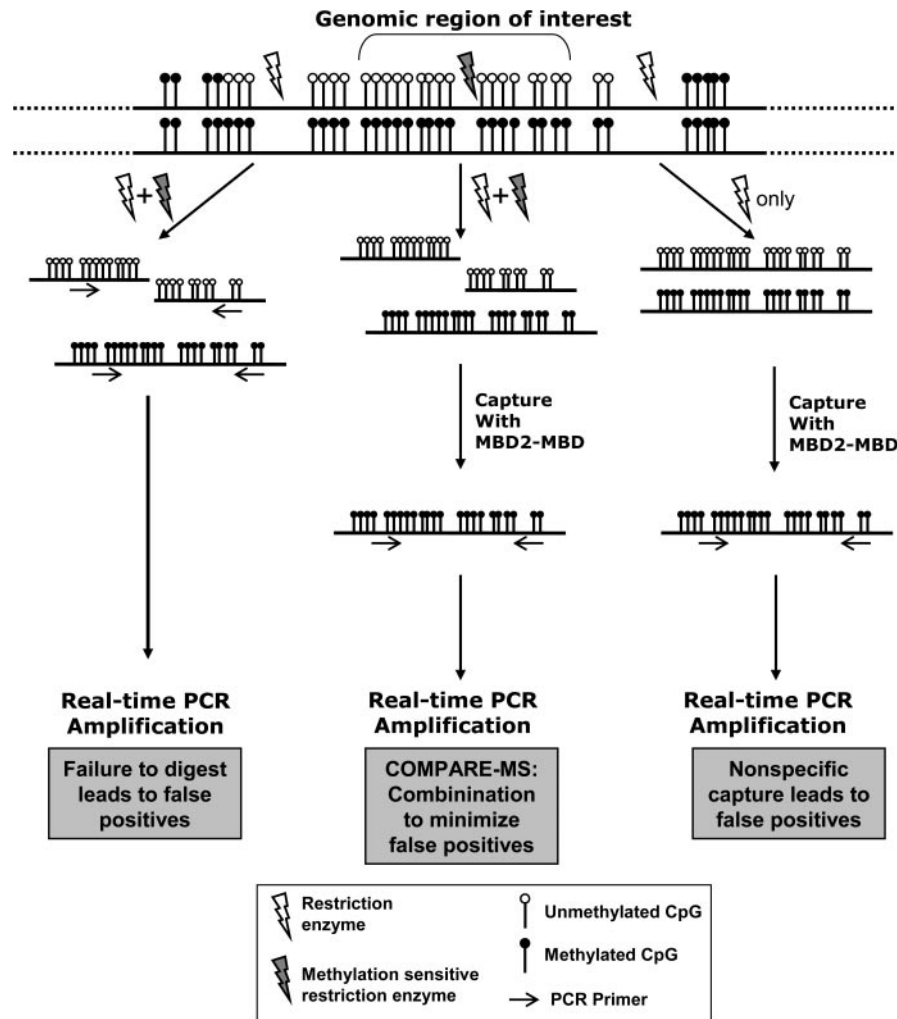
Figure 1. COMPARE-MS overview and rationale. Genomic DNA is digested with AluI with or without the methylation-sensitive restriction enzyme HpaII. After digestion, either the MBD2-MBD captured methylated DNA or all digested DNA are subjected to real-time PCR at a gene-specific locus. We hypothesized that enrichment of methylated DNA by methylation-sensitive restriction enzyme digestion alone or by MBD2-MBD capture of methylated DNA alone may result in false positives associated with incomplete digestion or nonspecific capture, respectively, while the combination of the two approaches (COMPARE-MS) would maintain sensitivity while minimizing false-positive results.

until further use. The final concentration of recombinant MBD2-MBD polypeptide was determined by the BCA assay (Pierce, Rockford, IL).

Fluorescence polarization analysis of MBD polypeptide binding to oligonucleotide substrates

Aliquots containing 10 nM of annealed, fluorescently labeled hairpin oligonucleotides with the sequence 5′-6FAM-ATCGTCGTACGTTTTCGTACGACGAT-3′ with no methylated CpGs (unmethylated hairpin), two methylated CpGs at the 2nd and 5th CpGs from the 5′ end (one symmetrically methylated CpG hairpin), three methylated CpGs toward the 3′ end (three asymmetrically methylated CpG hairpin), four methylated CpGs at the 1st, 2nd, 5th and 6th CpGs from the 5′ end (two symmetrically methylated CpG hairpin) or six methylated CpGs (three symmetrically methylated CpG hairpin) were incubated with varying concentrations of recombinant MBD2-MBD in a 50 μl reaction volume containing 4% glycerol, 1 mM MgCl$_2$, 0.5 mM EDTA, 0.5 mM DTT, 50 mM NaCl, 10 mM Tris–HCl (pH 7.4), 0.2% Tween-20 for 1 h at

room temperature with gentle shaking. Fluorescence polarization measurements were taken in triplicate using a Beckman Coulter DTX 880 Multimode Detector as described previously (35). Briefly, fluorescence anisotropies (*r*) were calculated as

$$r = (I_{\parallel} - I_{\perp})/(I_{\parallel} + 2I_{\perp})$$

where $I_{\parallel}$ represents the fluorescence intensity parallel to the incident light, $I_{\perp}$ represents the fluorescence intensity perpendicular to the incident light. In order to estimate the EC50, which is defined as the effective protein concentration required for binding 50% of the hairpin oligonucleotides, *r* was plotted against MBD2-MBD polypeptide concentration, and curve-fitted to a sigmoidal binding curve using Sigma Plot 8.0 (Systat Software, Richmond, CA).

COMPARE-MS assay and real-time PCR

An overview of the COMPARE-MS assay is shown in Figure 1. DNA samples were digested at 37°C for 3 h with 15 U AluI (NEB, Beverly, MA) with or without 15 U of HpaII

Table 1. PCR primers used in COMPARE-MS assay

| Gene symbol	Forward primer	Reverse primer
GSTP1	5′-GGGACCCTCCAGAAGAGC	5′-ACTCACTGGTGGCGAAGACT
PTGS2 (COX2)	5′-GGAGAGGAAGCCAAGTGTCC	5′-GGTTTCCGCCAGATGTCTTT
MDR1 (ABCB1)	5′-GTGGGTGGGAGGAAGCAT	5′-TCTCCAGCATCTCCACGAAG
ESR1	5′-CTCGGGCTGTGCTCTTTTTC	5′-CCAGATGCTTTGGTGTGGAG
DAPK1	5′-CTTGCAGGGTCCCCATTG	5′-GTCCGGCTGTCCTCCTCA
CDH1	5′-CAGGTGAACCCTCAGCCAAT	5′-CACAGGTGCTTTGCAGTTCC
LINE1	5′-CGCAGAAGACGGGTGATTTC	5′-CCGTCACCCCTTTCTTTGAC
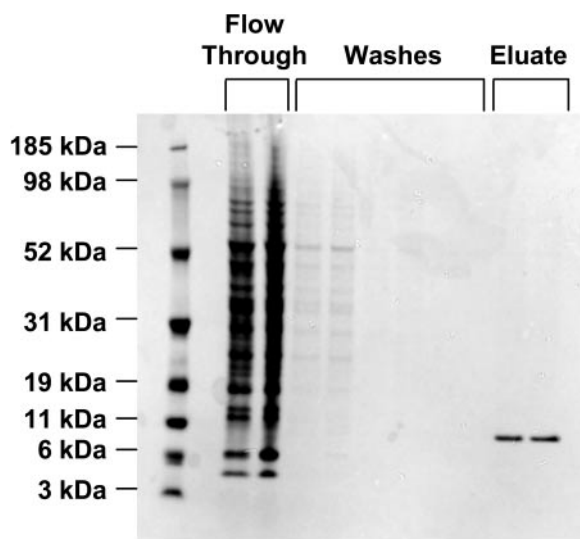
Figure 2. Baculovirus-mediated expression of C-terminal His_6-tagged human MBD2-MBD in Sf9 insect cells and purification by Ni-NTA beads. Unbound lysate, washes and eluted purified protein were run on an SDS–PAGE gel and stained with Coomassie Blue R-250. The eluate contained the purified ~9.8 kDa MBD2-MBD-His_6.

(NEB, Beverly, MA). After digestion, restriction enzymes were heat inactivated at 65°C for 30 min. Aliquots containing 2.5 µl of Protein G Magnetic Beads (NEB, Beverly, MA) were gently shaken for 1 h at room temperature with 1 µg of PentaHis Antibody (Qiagen, Valencia, CA), 160 nM MBD2-MBD-His_6 and 200 ng of an unmethylated self-ligated TOPO-TA plasmid (Invitrogen, Carlsbad, CA), in 97.5 µl of BW Buffer [4% glycerol, 1 mM $MgCl_2$, 0.5 mM EDTA, 0.5 mM DTT, 50 mM NaCl, 10 mM Tris–HCl (pH 7.4), 0.2% Tween-20 and 1× Complete EDTA-free Protease Inhibitor cocktail]. Unbound antibody and MBD polypeptides were removed by immobilizing beads on a Magnetight HT96 magnetic rack (Novagen, San Diego, CA) and removing the supernatant. Restriction enzyme digested DNA samples were diluted in 100 µl of BW buffer and then incubated with the beads for 1 h at room temperature with gentle shaking. The beads were then immobilized on the Magnetight HT96 rack and washed five times with BW Buffer. After the final wash, 20 µl of 1 mM Tris–HCl (pH 8.0) was added and the reaction was heated to 95°C for 15 min to elute the DNA. The magnets were again immobilized on the Magnetight HT96 rack and the supernatant containing the released DNA was removed and stored at −20°C until further use. These DNA samples were then subjected to real-time PCR in 50 µl reaction volumes containing 1× IQ SYBR Green Supermix (Biorad, Hercules, CA), and 400 nM forward and reverse primers. Primer

sequences for assayed CGIs are shown in Table 1. PCRs consisted of a 95°C denaturing step for 10 min, followed by 45 cycles of 94°C for 30 s, 60°C for 30 s with real-time detection and 72°C for 30 s. All assays were carried out in duplicates or triplicates. All real-time PCR amplicons contained at least one HpaII restriction enzyme site. M.SssI (NEB) treated male WBC genomic DNA served as a positive control for all CGIs while untreated male WBC genomic DNA served as a negative control. The completion of the M.SssI methyltransferase reaction was verified by showing that the treated DNA could not be fragmented by HpaII restriction enzyme and that all CpGs at the *GSTP1* promoter CGI were methylated by bisulfite genomic sequencing (36) (data not shown). For prostate cell lines and tissues, methylation levels were normalized to the signal generated by an equal input amount of the positive control to generate a methylation index (MI), which was displayed using a color scale in which red indicates MI > 0.99 and white indicates MI = 0. Because a quantitative internal control could not be used for each sample, it is important to note that accurate quantitation of DNA in each sample prior to COMPARE-MS analysis is crucial to the accuracy of COMPARE-MS. In this study, DNA quantitation of all samples was performed prior to restriction enzyme digestion and MBD2-MBD capture by UV absorbance and by real-time PCR of the Beta-globin gene. In the few samples in which there was a discrepancy between the absorbance and real-time PCR derived quantities, the real-time PCR quantity was used since this would be a better estimate of amplifiable DNA. As a post-analysis quality check, for specimens that had no detectable signals at all CGIs tested by COMPARE-MS, real-time PCR amplification of LINE1 repetitive elements, which are methylated to a large extent in human genomic DNA, using primers complementary to the LINE1 promoter consensus sequence (GenBank accession X58075), was performed to ensure that recovery of methylated DNA was not compromised during COMPARE-MS (data not shown).

Bisulfite genomic sequencing

An aliquot of 500 ng of genomic DNA was bisulfite converted using the EZ DNA methylation kit (Zymo Research, Orange, CA) and eluted in 10 µl of TE buffer, pH 7.4. Primers amplifying *GSTP1* CpG islands without bias to methylation patterns were forward primer, 5′-GTTGGTTTTATGTTGGGAGTTTTGAGTTTT; reverse primer, 5′-ATCCTCTTCCTAC-TATCTATTTACTCCCTAA. PCR was carried out in 40 µl reactions containing 1 µl of bisulfite converted DNA, 1× Platinum *Taq* buffer (Invitrogen, Carlsbad, CA), 1.5 U Platinum *Taq* (Invitrogen), 250 µM each dNTPs, 1.5 mM
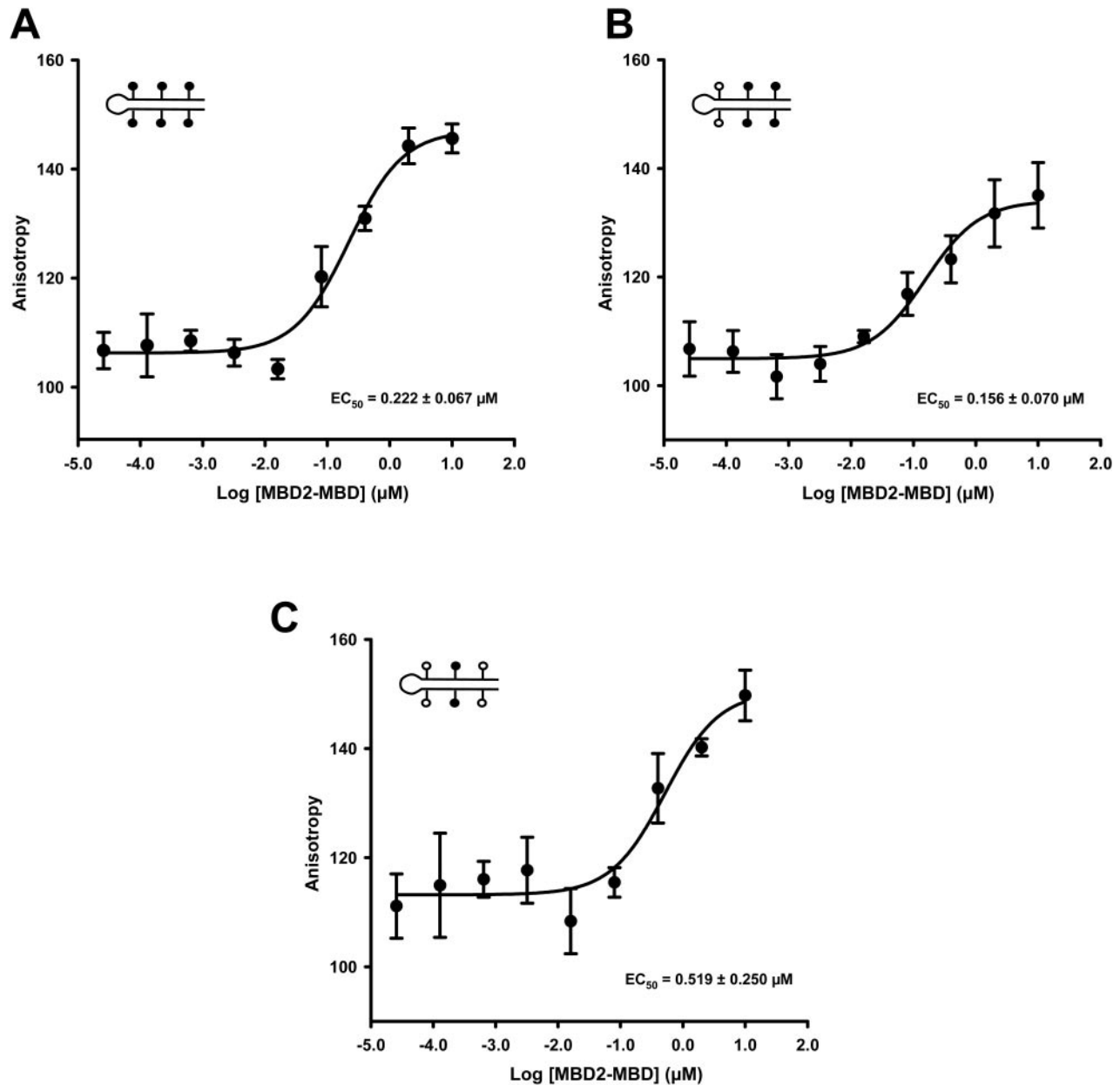
Figure 3. Determination of MBD2-MBD affinity for symmetrically methylated hairpin olignucleotide ligands. (**A–C**) Fluorescence anisotropy measurements were plotted as a function of MBD2-MBD concentration in order to estimate the relative affinity of MBD2-MBD for fluorescently labeled hairpin oligonucleotides containing three pairs (A), two pairs (B) and one pair (C) of symmetrically methylated CpG dinucleotides. The EC_{50}, defined as the MBD2-MBD concentration required to achieve half maximal binding of 10 nM hairpin oligonucleotides, is shown for each case, along with the corresponding SEM. Data shown represent mean ± SEM for triplicate measurements.

MgCl$_2$, 0.25 µg/µl BSA, 2 µl dimethyl sulfoxide, 400 nM forward primer and 400 nM reverse primer. Cycling conditions were 95°C for 3 min, 35 cycles of 95°C for 30 s, 50°C for 30 s and 72°C for 30 s, followed by a 7 min extension step at 72°C. PCR products were gel purified after electrophoresis on a 1% agarose gel, sub-cloned into pCR®2.1-TOPO® vector (Invitrogen) and analyzed by dideoxy sequencing.

Statistical analysis

Receiver operator characteristic (ROC) curves were generated using MedCalc (Mariakerke, Belgium) by plotting sensitivity (%) versus 100-specificity (%) for varying MI thresholds. The 130 primary prostate cancer tissues were defined as true positives while the 13 benign prostate tissues from organ donors were designated true negatives. These curves were used to determine the MI threshold that yields the optimal sensitivity and specificity. Area under the ROC curves (AUC) and their 95% confidence intervals were found. The AUC represents the probability that a randomly chosen sample from the true positives group will have an MI that is greater than a randomly chosen sample from the true negatives group. All error bars shown in this study represent SEM.
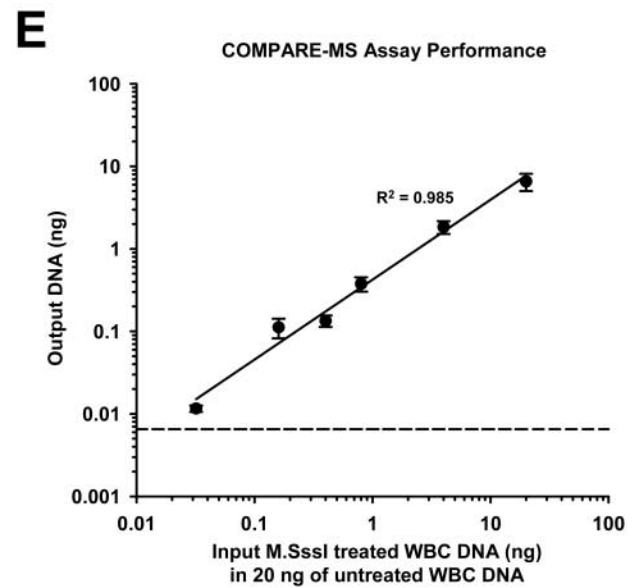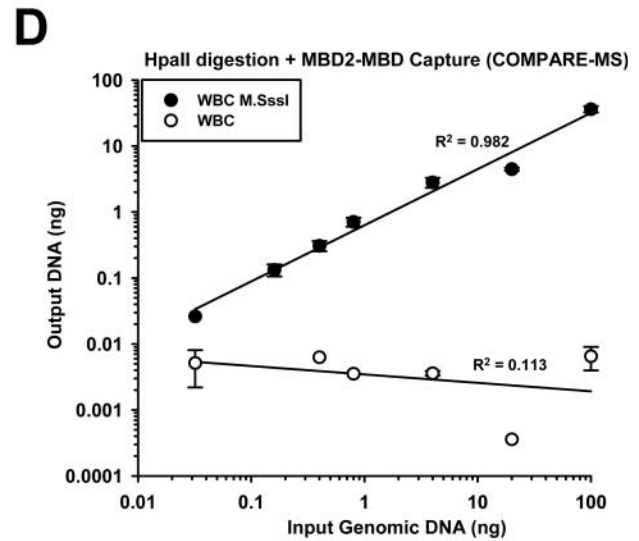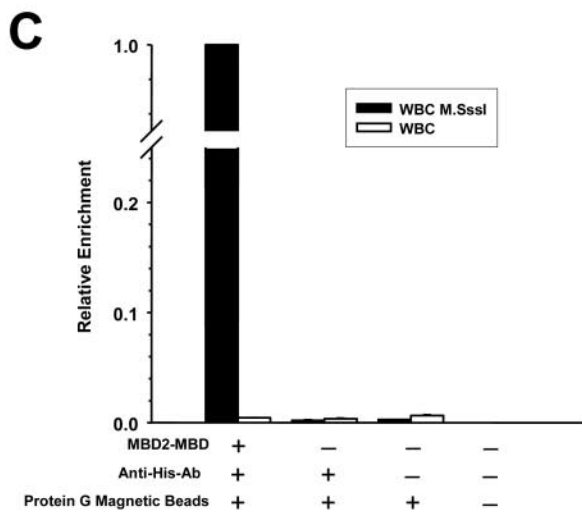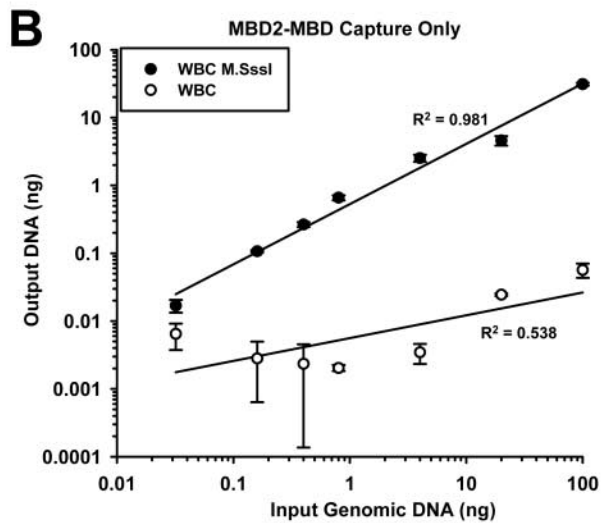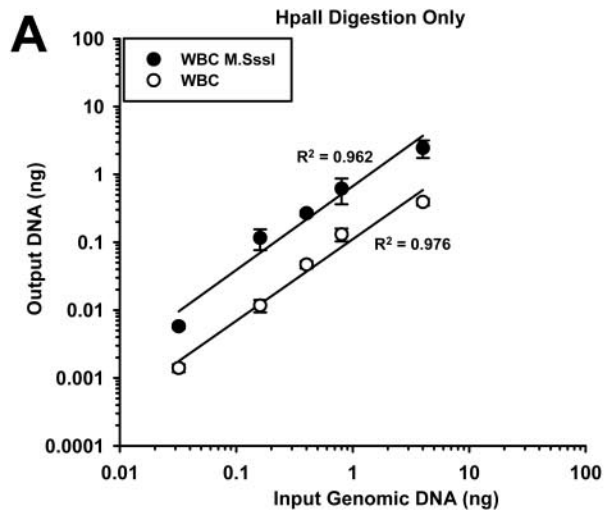
COMPARE-MS assay performance linear regression analysis was performed with SigmaPlot 8.0.

RESULTS

Fluorescence anisotropy measurements for the estimation of MBD2-MBD affinity for various DNA templates

His$_6$-tagged MBD of human MBD2 (MBD2-MBD) was expressed in Sf9 insect cells using a baculoviral expression system and purified using Ni-NTA Superflow beads (Qiagen, Valencia, CA) (Figure 2). The affinities of MBD2-MBD for fluorescently labeled hairpin oligonucleotides containing various configurations of CpG methylation were then determined by fluorescence polarization (Figure 3). The EC50 for MBD2-MBD binding to hairpin oligonucleotides containing two or three symmetrically methylated CpGs was 156 and 222 nM, respectively (Figure 3A and B). For hairpin oligonucleotides with a single symmetrically methylated CpG (Figure 3C) the EC50 = 519 nM. In contrast, the MBD2-MBD did not bind asymmetrically methylated and unmethylated hairpin oligonucleotides to any appreciable extent in the concentration range tested suggesting that the EC50 $\gg$ 10 μM for these ligands (data not shown). The high affinity and specificity of MBD2-MBD for symmetrically methylated DNA made it ideal for enrichment and capture of methylated DNA from heterogeneous samples.

Dynamic range of detection of methylated *GSTP1* CGIs by COMPARE-MS and each of its components individually

We compared the abilities of digestion with a methylation-sensitive restriction enzyme alone, MBD2-MBD capture of methylated DNA alone, and the combination of the two approaches in distinguishing between methylated and unmethylated *GSTP1* promoter CGIs (Figure 4). Genomic DNA containing completely methylated *GSTP1* promoter CGIs was generated by treating WBC genomic DNA, which is normally unmethylated at this CGI, with M.SssI DNA methyltransferase. In an ideal methylation assay, 100% of the M.SssI-treated DNA would be detected while the amount of falsely detected untreated WBC DNA would diminish to zero. For this scenario, the dynamic range, defined as the amount of methylated alleles detected in the M.SssI-treated DNA divided by the amount falsely detected in the untreated WBC DNA, would approach infinity.

HpaII restriction enzyme digestion followed by real-time PCR with primers flanking a single recognition site achieved a dynamic range of $\sim$6- to 10-fold at all concentrations of input DNA tested (Figure 4A). These data are in agreement with a previous study showing a dynamic range of $\sim$10-fold when the amplicon contains one HpaII recognition sequence (21). MBD2-MBD capture of methylated DNA alone followed by real-time PCR showed a maximum dynamic range of $\sim$500- to 700-fold at high (4–100 ng) input DNA amounts steadily decreasing to a minimum dynamic range of approximately 3- to 10-fold at low (32 pg) input DNA amounts (Figure 4B). At high concentrations of input DNA, a small amount of untreated WBC DNA was detected above background, but this was likely due to nonspecific binding of the unmethylated DNA to the beads as opposed to specific binding of unmethylated DNA to the MBD2-MBD, since the same amount of background DNA capture occurred even in the absence of MBD2-MBD (Figure 4C). When input DNA was first cut with HpaII, then precipitated with the MBD2-MBD, and finally subjected to real-time PCR, the maximum dynamic range was $\sim$5000- to 10 000-fold with 20–100 ng input DNA, decreasing to 10-fold at 32 pg (5–6 genomic equivalents) input DNA (Figure 4D). Therefore, the combination of these techniques, termed COMPARE-MS, is superior to either technique used alone. Furthermore, the ability to detect hypermethylated *GSTP1* CGIs was highly linear ($R^2 = 0.982$) over a 3125-fold range of input DNA. In contrast, the signals from unmethylated DNA templates were uniformly low and unrelated to input DNA amount ($R^2 = 0.113$), suggesting that these low signals were due to the random noise in the assay, likely resulting from carrying out high cycle numbers in real-time PCR.

In sum, the COMPARE-MS assay could allow reliable quantitation of methylated CGIs even when only 0.03% or 1/3125 of input alleles are methylated. This sensitivity and specificity could allow accurate detection of hypermethylated cancer DNA in >1000-fold excess unmethylated normal DNA, as would be found in heterogeneous DNA samples obtained from non-dissected tissues, biopsy specimens and bodily fluids.

COMPARE-MS assay performance in simulated heterogeneous samples

To test this potential more directly, we examined the COMPARE-MS assay's performance by using it to analyze samples containing decreasing amounts (20 ng–32 pg) of

Figure 4. COMPARE-MS assay performance. (**A** and **B**) Plots showing the measured amount of methylated *GSTP1* CGIs in M.SssI treated and untreated WBC genomic DNA versus the amount of input DNA after enriching for methylated DNA by methylation-sensitive restriction enzymes alone (A) or MBD2-MBD capture alone (B). (**C**) Plot of relative enrichment of M.SssI treated or untreated WBC DNA with or without MBD2-MBD, anti-His antibody and protein G magnetic beads. The degree of capture of unmethylated DNA (untreated WBC DNA) in the presence of MBD2-MBD is less than or equal to the capture of DNA in the absence of MBD2-MBD or anti-His antibody, showing that capture of unmethylated DNA during the DNA capture step of COMPARE-MS is almost completely due to low amounts of non-specific binding to the protein G magnetic beads, as opposed to low-level binding of the MBD2-MBD to unmethylated DNA. (**D**) Plots showing the measured amount of methylated *GSTP1* CGIs in M.SssI treated and untreated WBC genomic DNA versus the amount of input DNA after enriching for methylated DNA by the combination of methylation-sensitive restriction enzyme digestion and MBD2-MBD capture (COMPARE-MS) followed by real-time PCR. When 20–100 ng of input DNA are used, COMPARE-MS has a >5000-fold dynamic range, which is $\sim$500-fold higher than that of methylation-sensitive restriction enzyme used alone and $\sim$5- to 10-fold higher than that of MBD2-MBD capture used alone. (**E**) Plot showing measured output methylated *GSTP1* CGIs as determined by COMPARE-MS when decreasing amounts of M.SssI-treated WBC DNA are diluted in 20 ng of untreated WBC genomic DNA. The dashed line is a reference representing the mean COMPARE-MS output (0.0065 ± 0.0023 ng) when four identical replicates of 100 ng of untreated, unmixed WBC genomic DNA were analyzed. COMPARE-MS performance in this series of simulated heterogeneous samples (E) is highly linear for almost four orders of magnitude and nearly identical to that seen with homogeneously methylated samples (D), showing robust reproducibility and sensitivity. Data in (A–E) represent mean ± SEM for triplicate measurements.

RT-MSP primer and probe binding sites

COMPARE-MS PCR amplicon with HpaII site indicated

Unmethylated CpG

Transcriptional start

GSTP1 promoter with CpG sites indicated

Methylated CpG

M.SssI-treated WBC genomic DNA diluted in a fixed amount (20 ng) of untreated WBC DNA (Figure 4E). These mixtures are a simulation of heterogeneous samples. We used a fixed amount of 20 ng of untreated WBC genomic DNA because this represents a realistic amount we would want to input to actual COMPARE-MS assays in order to conserve DNA specimens. As anticipated by the dynamic range studies, the COMPARE-MS assay had a linear quantitative response ($R^2 = 0.985$) over a broad dilution range spanning more than three orders of magnitude. Furthermore, the assay performance in samples diluted in excess unmethylated DNA was extremely similar to the performance in samples containing pure methylated DNA (Figure 4D and E). The COMPARE-MS assay could reliably detect 32 pg (5–6 cells) of methylated DNA without being overwhelmed by the 625-fold excess of unmethylated genomic DNA. The same reliability in quantitation was achieved when 32 pg of methylated DNA was diluted in 100 ng ($\sim$3125-fold) of excess unmethylated DNA (data not shown), confirming that accurate quantitation of *GSTP1* CGI hypermethylation could be achieved in mixtures containing 625- to 3125-fold excess contaminating unmethylated DNA.

CGI hypermethylation profile of prostate cancer cell lines by COMPARE-MS

COMPARE-MS was used to assess the quantity of hypermethylated CGI sequences at six cancer-related genes in six prostate cancer cell lines and normal prostate epithelial cells (PrECs) in primary culture (Figure 5). CGI sequences at *GSTP1*, *PTGS2* and *MDR1* were found to be frequently and prevalently methylated in multiple prostate cancer cell lines. The *ESR1* CGI was highly methylated in PC-3 cells, slightly methylated in the DU-145 cells, but unmethylated in the other cell lines. The CGI at *DAPK1* was methylated to a small extent in the PC-3 cell line. The *CDH1* CGI was not methylated at any of the prostate cancer cell lines. PrECs and WBCs were not methylated at any of the CGIs tested. These experiments demonstrate the general applicability of the COMPARE-MS assay to CGIs at multiple genes (Figure 5A). With few exceptions, the CGI methylation pattern in these cells determined by COMPARE-MS is extremely similar to the pattern determined by MethyLight (Figure 5A and B) in a previous study (33). Among the exceptions, the MethyLight study did not detect any *GSTP1* CGI hypermethylation in CWR22Rv1, while COMPARE-MS detected a significant amount of methylated GSTP1 CGI alleles in this cell line. To test the accuracy of the COMPARE-MS assay, we performed bisulfite genomic sequencing of the *GSTP1* CGI in DNA from CWR22RV1, LNCaP and PrEC cells (Figure 5C). This

analysis showed that COMPARE-MS was accurate in predicting a high degree of *GSTP1* CGI hypermethylation in the CWR22Rv1 cell line (MI = 0.71). As seen by the bisulfite sequencing data, the reason that MethyLight could not detect any GSTP1 CGI hypermethylation in this sample is most likely that many of the CpGs interrogated by the MethyLight primers and probe were unmethylated in almost all of the alleles. However, the ability of the COMPARE-MS assay to correctly detect a high degree of hypermethylation at the CWR22Rv1 was somewhat fortuitous since the HpaII site interrogated by the COMPARE-MS assay was highly methylated in this cell line. For instance, when using a different set of real-time PCR primers that flank a single SmaI site at the 11th CpG upstream of the −266 position of the GSTP1 promoter (indicated in Figure 5C), the COMPARE-MS assay detects a very low (MI = 0.031), but greater than background degree of hypermethylation (data not shown). Additionally, when WBC DNA was partially methylated by M.HhaI and M.HpaII at nine CpG sites (24% of all CpG sites) within the AluI fragment interrogated by the COMPARE-MS assay, we detected just a small, but greater than background, fraction of input alleles (MI = 0.036) compared with an equivalent input amount of M.SssI methylated WBC DNA (data not shown). Therefore, the dynamic range and diagnostic sensitivity of COMPARE-MS would be limited if the CpGs interrogated by the methylation-sensitive restriction enzyme is highly under-methylated compared with the surrounding CpGs or if there is a low density of methylation in the interrogated AluI fragment. This limitation is not unlike that for MSP and MethyLight when the CpGs interrogated by the methylation-specific primers and probes are undermethylated compared with the surrounding CpGs or when there is a low density of methylation at the interrogated CpGs.

Detection of CGI hypermethylation by COMPARE-MS in prostate cancer and benign prostate tissues

To test its performance on heterogeneous human tissues, the COMPARE-MS assay was used to determine the extent of methylation at the *GSTP1*, *PTGS2*, *MDR1* and *ESR1* CGIs in benign prostate tissues from 13 transplant organ donors, prostate cancer tissues from 130 men undergoing radical prostatectomy for treatment of localized prostate cancer and tumor-adjacent benign prostate cancer tissues microdissected from 12 of the 130 men undergoing radical prostatectomy (Figure 6). We chose tissues such that a large subset of the prostate cancer tissues analyzed in this study were analyzed by MethyLight previously (33). Similar to the prostate cancer cell lines, the CGIs at *GSTP1* (99.2%), *MDR1* (95.4%) and *PTGS2*

Figure 5. Validation of COMPARE-MS by analysis of hypermethylation at six gene-specific CGIs in multiple prostate cell lines. (**A**) Methylation index (MI), defined as the ratio of the amount of methylated alleles in a given sample to the amount of methylated alleles in the same input quantity of M.SssI-treated WBC DNA, as determined by COMPARE-MS, for six cancer-related genes (*GSTP1*, *PTGS2*, *MDR1*, *ESR1*, *DAPK1* and *CDH1*) in 20 ng of genomic DNA from six prostate cancer cell lines (LNCaP, C42B, PC-3, DU-145, LAPC-4 and CWR22Rv1), one primary culture model of non-malignant prostate epithelial cells (PrEC) and untreated WBC negative control. (**B**) MI for the same set of CGIs and samples as determined by MethyLight in a previous study (33). With few exceptions, the CGI hypermethylation pattern obtained from COMPARE-MS (A) is highly similar to those obtained from MethyLight (B). Asterisk denotes MI <0.2 but at least 3 SD greater than the background level seen in 10 identical replicates of WBC samples. These data demonstrate the applicability of COMPARE-MS to multiple genes and heterogeneous samples. (**C**) Bisulfite genomic sequencing of the *GSTP1* CGI in PrEC, LNCaP and CWR22Rv1 cell lines. Bisulfite sequencing shows that COMPARE-MS was accurate in identifying that the *GSTP1* CGI in CWR22Rv1 cells is highly methylated, and demonstrates that MethyLight failed to detect this because many of the CpG dinucleotides interrogated by the methylation specific primers and probe were mostly unmethylated. Both COMPARE-MS and MethyLight were able to correctly identify that LNCaP and PrEC cells were homogeneously methylated and unmethylated, respectively. The indicated bisulfite sequencing start and end positions are relative to the transcriptional start site.
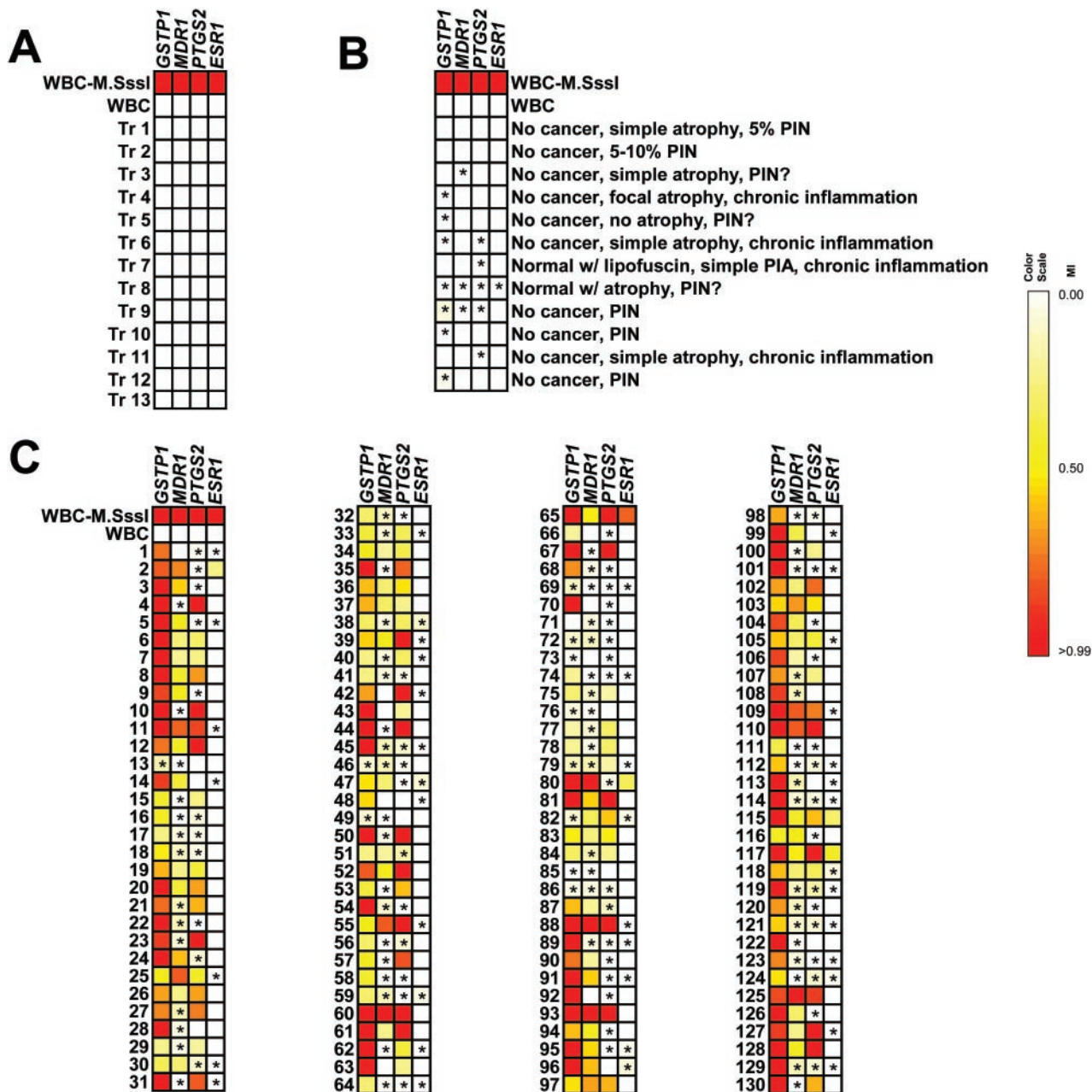
Figure 6. COMPARE-MS applied to heterogeneous prostate tissues. (**A–C**) MI at the *GSTP1*, *MDR1*, *PTGS2* and *ESR1* CGIs in 20 ng of genomic DNA from benign prostate tissues obtained from 13 organ donors, who had no evidence of prostatic malignancies (A), 20 ng of genomic DNA from tumor-adjacent benign prostate cancer tissues isolated from 12 of the 130 men from whom prostates were obtained during radical prostatectomy for treatment of primary prostate cancer (B) and 20 ng of genomic DNA from primary prostate cancer tissues from 130 primary prostate cancer patients undergoing radical prostatectomy for treatment of their disease (C). Asterisk denotes MI <0.2 but greater than the threshold determined by ROC curve analysis. These data demonstrate the applicability of COMPARE-MS to heterogeneous human tissue samples.

(95.4%) were hypermethylated in a large percentage of the 130 primary prostate cancer specimens and had, on average, a high prevalence of methylated copies (mean and median MI > 0.15). The *ESR1* CGI was methylated in 47.7% of the primary prostate cancers with a low, but above-threshold, prevalence (mean and median MI < 0.03). In contrast, benign prostate tissues from organ donors, who did not have evidence of prostatic malignancies, had undetectable methylation at these CGIs. Interestingly, many of the tumor-adjacent benign tissues exhibited a low (mean and median MI < 0.02), but

above threshold, amount of CGI hypermethylation at the *GSTP1*, *MDR1* and *PTGS2* genes (frequency of 58.3, 25 and 50%, respectively). A much smaller percentage of these tissues had detectable CGI hypermethylation by the MethyLight assay (33). ROC curves were used to analyze the optimal sensitivity and specificity of *GSTP1*, *MDR1* and *PTGS2* CGI CGI hypermethylation as determined by the COMPARE-MS assay in differentiating primary prostate cancer from benign prostate (Figure 7). Hypermethylation of all three of these CGIs could achieve sensitivities >95% and specificities
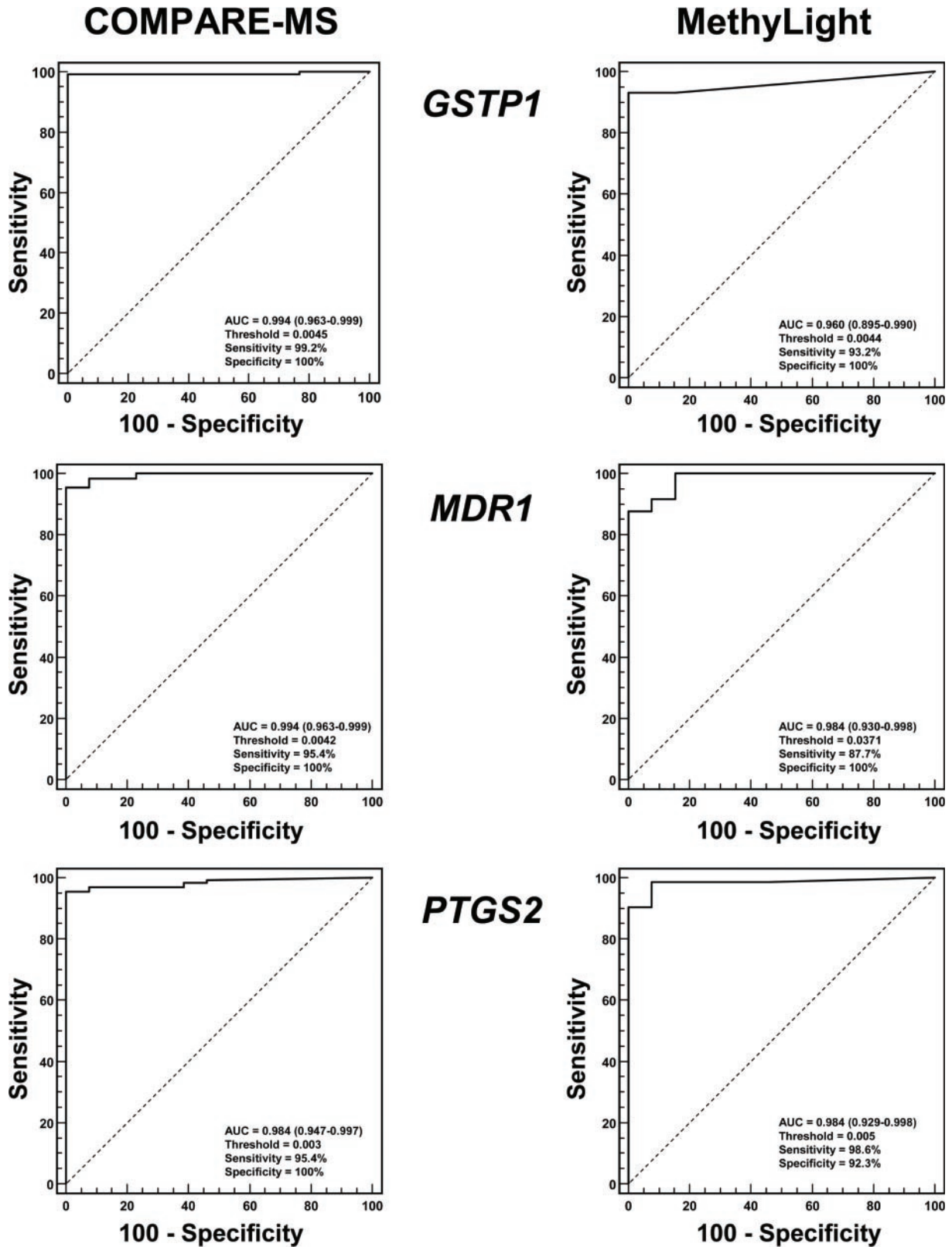
Figure 7. Comparison of ROC curves obtained by COMPARE-MS with those obtained by MethyLight. ROC curves for hypermethylation at the *GSTP1*, *MDR1* and *PTGS2* CGIs in distinguishing between benign and malignant prostate as determined by COMPARE-MS were comparable with those generated by MethyLight (33). An ideal assay would perfectly distinguish between true positives and true negatives and would have an area under the ROC curve of 1.0. The dashed lines represent the ROC curve for a hypothetical test that cannot distinguish between these two groups, giving an AUC of 0.5. CGI hypermethylation at the *GSTP1*, *MDR1* and *PTGS2* genes as determined by COMPARE-MS distinguish benign prostate from prostate cancer with high sensitivity and specificity, with AUCs extremely close to the ideal case.

approaching 100%. The areas under the ROC curves (AUC) for these CGIs as determined by COMPARE-MS approached 1.0 and were comparable with those determined by MethyLight (33). Interestingly, four out of the five prostate cancer cases that had undetectable *GSTP1* CGI hypermethylation by MethyLight were found to be hypermethylated by the COMPARE-MS assay. Furthermore, the one prostate cancer case that had undetectable *GSPT1* CGI hypermethylation by the COMPARE-MS assay was also undetectable by MethyLight. Taken together, these data demonstrate the applicability of the COMPARE-MS assay for the sensitive, specific and rapid identification of aberrant CGI hypermethylation in heterogeneous tissues.

DISCUSSION

This report describes a novel DNA methylation assay called COMPARE-MS that greatly enriches for methylated DNA in heterogeneous samples by combining two independent and complementary strategies: (i) digestion with methylation-sensitive restriction enzymes and (ii) specific capture of methylated DNA by binding to MBD polypeptides immobilized on a magnetic solid matrix. The enriched methylated DNA is then subjected to gene-specific quantitative PCR to determine quantities of methylated CGIs in DNA from heterogeneous samples. One significant advantage of COMPARE-MS over previous methods is that it does not require sodium bisulfite modification. For the methylation-sensitive restriction enzyme step of COMPARE-MS, we chose to use HpaII because its recognition site is abundant in most CGIs. Other methylation-sensitive restriction enzymes may be equally effective. The second step of COMPARE-MS, capture and enrichment of methylated DNA fragments, is similar to the previously reported MIRA (26), MeDIP (32) and MECP2-MBD column (23–25) based assays. In particular, the methylated-DNA capture step of COMPARE-MS is similar to the MIRA assay, which uses full-length GST-tagged-MBD2-bound magnetic beads for affinity purification of methylated DNA fragments. However, one notable difference between the methylated-DNA capture step of COMPARE-MS and these previous techniques is that we used the small, ~10 kDa MBD fragment of MBD2 for affinity capture and enrichment of methylated DNA fragments, while the MIRA, MeDIP and MECP2-MBD column-based assays used full-length MBD2, α5mC-Abs or the MBD fragment of MECP2, respectively. The use of MBD2-MBD in COMPARE-MS may provide significant advantages over these other reagents for the capture and enrichment of methylated DNA. First, we show that the MBD2-MBD has high affinity and specificity for symmetrically methylated DNA templates. Previous studies have also shown that of all the MBD proteins, MBD2 has the highest affinity for a wide range of methylated DNA sequences (37), while MECP2 may selectively bind to CpG dinucleotides adjacent to A/T-rich sequences (38). Second, because it binds double-stranded methylated DNA, MBD2-MBD may be a better candidate for enrichment of CGIs than the α5mC-Abs which only bind single-stranded DNA (32). This is an especially important consideration since the high G/C content of CGIs may make these sequences resistant to denaturing and prone to forming

secondary structures even after denaturing. Finally, using just the small ~10 kDa MBD portion of the MBD2 protein, as opposed to the full-length protein, could eliminate unwanted interactions between unmethylated DNA and other domains on the MBD2 protein. In this study, enrichment of methylated DNA by the combination of digestion with HpaII and capture with the MBD2-MBD minimized the rate of false positives, while maintaining exquisite sensitivity. Furthermore, these processes involve minimal 'hands-on' time and small reaction volumes, making COMPARE-MS highly compatible with automated, high-throughput, micro-titer plate analysis. After the initial assay development and optimization stages, we determined the methylation pattern of >160 prostate tissue and cell line samples at multiple CGIs in a single day.

This analysis showed that the CGI hypermethylation pattern at *GSTP1*, *PTGS2* and *MDR1* could identify prostate cancer with sensitivities >95% and specificities approaching 100%. Furthermore, we showed that the sensitivity, specificity and dynamic range achieved by COMPARE-MS are highly comparable with those reported for MSP, MethyLight and HeavyMethyl. However, unlike these other techniques, COMPARE-MS is not encumbered with the disadvantages of sodium bisulfite modification. This may allow for higher compatibility with high-throughput, automated, micro-titre-based platforms, and greater ease in the design of real-time PCR primers since there is no reduction in genome sequence complexity. Also, typically, MSP and MethyLight identify the prevalence of a single pattern of methylation at the CpG dinucleotides interrogated by the primers and probes. Although theoretically it may be possible to carry out multiple reactions, each interrogating a different pattern and different set of CpGs, the low sequence complexity of bisulfite-treated DNA limits the application of such strategies. COMPARE-MS, on the other hand, was designed to detect a broader range of abnormal methylation patterns across a large set of CpG dinucleotides without significant design limitations. This feature of COMPARE-MS can be viewed as both a strength and a weakness.

On the one hand, this difference between COMPARE-MS versus MSP and MethyLight may be the reason that four out of the five primary prostate cancer cases in which MethyLight could not detect any *GSTP1* CGI hypermethylation were detected by the COMPARE-MS assay. More provocatively, a larger fraction of the tumor-adjacent benign prostate tissues had a small, but significant, amount of methylated CGIs at the *GSTP1*, *PTGS2* and *MDR1* genes when analyzed by COMPARE-MS than when analyzed by MethyLight. This finding is in agreement with a recent study showing that the normal epithelia and stroma in tumor-adjacent benign tissues in breast cancers displayed significant hypermethylation of CpG islands (39). Most of the tumor-adjacent benign tissues in this study had some prostatic intraepithelial neoplasia (PIN) and/or proliferative inflammatory atrophy lesions, which have been shown to have some methylation at the *GSTP1* CGI by MSP, but only after rigorous purification of these cells by laser capture microdissection (LCM) (34). In this study, even without LCM, we were able to quantitatively detect trace amounts of hypermethylation at these CGIs by COMPARE-MS, illustrating the utility of this technique in highly heterogeneous tissues containing only a small amount of methylated DNA. However, since LCM was not used, we could not rule out the

possibility that the detected DNA hypermethylation was due to trace contamination by cancer cells. Larger studies, using LCM in at least a subset of samples, would have to be performed to verify this finding.

On the other hand, the ability to detect a broader range of methylation patterns is also a limitation of COMPARE-MS, because it would not be able to quantitate the prevalence of specific patterns of CpG dinucleotide methylation in a given sample. The role of COMPARE-MS would therefore be to quantitate the degree of aberrant hypermethylation with high sensitivity, specificity and rapidity. If necessary, specific samples of interest, as identified by COMPARE-MS, can then be studied by the use of other techniques such as bisulfite genomic sequencing (36) for determination of the prevalence of specific patterns of DNA methylation.

The COMPARE-MS assay, or components of it, may also be useful for many different methylation detection applications that were not explored in this study. First of all, its sensitivity, specificity and ease of use would allow for design of large clinical trials testing the efficacy of DNA methylation patterns in the diagnosis and risk stratification of human diseases, including cancer. Additionally, since COMPARE-MS does not involve bisulfite modification of the DNA, the original DNA sequence complexity is preserved. Consequently, multiplexing methylation detection at several CGIs in a single assay may be possible. Also, COMPARE-MS may be modified slightly to allow unbiased detection of novel methylated regions by a number of strategies including microarray hybridization (32,40,41), digital karyotyping (39), restriction fragment length genome scanning (42), etc. The use of COMPARE-MS could not only enhance our understanding of the role of DNA methylation in health and disease, but improve our ability to sensitively, specifically and rapidly detect CGI hypermethylation.

ACKNOWLEDGEMENTS

REFERENCES

1. Li,E., Bestor,T.H. and Jaenisch,R. (1992) Targeted mutation of the DNA methyltransferase gene results in embryonic lethality. *Cell*, **69**, 915–926.
2. Lande-Diner,L. and Cedar,H. (2005) Silence of the genes–mechanisms of long-term repression. *Nature Rev. Genet.*, **6**, 648–654.
3. Bird,A. (2002) DNA methylation patterns and epigenetic memory. *Genes Dev.*, **16**, 6–21.
4. Walsh,C.P., Chaillet,J.R. and Bestor,T.H. (1998) Transcription of IAP endogenous retroviruses is constrained by cytosine methylation. *Nature Genet.*, **20**, 116–117.
5. Antequera,F. and Bird,A. (1993) Number of CpG islands and genes in human and mouse. *Proc. Natl Acad. Sci. USA*, **90**, 11995–11999.
6. Jones,P.A. and Baylin,S.B. (2002) The fundamental role of epigenetic events in cancer. *Nature Rev. Genet.*, **3**, 415–428.
7. Esteller,M., Corn,P.G., Baylin,S.B. and Herman,J.G. (2001) A gene hypermethylation profile of human cancer. *Cancer Res.*, **61**, 3225–3229.
8. Issa,J.P. (2004) CpG island methylator phenotype in cancer. *Nature Rev. Cancer*, **4**, 988–993.
9. Laird,P.W. (2003) The power and the promise of DNA methylation markers. *Nature Rev. Cancer*, **3**, 253–266.
10. Belinsky,S.A. (2004) Gene-promoter hypermethylation as a biomarker in lung cancer. *Nature Rev. Cancer*, **4**, 707–717.
11. Wang,R.Y., Gehrke,C.W. and Ehrlich,M. (1980) Comparison of bisulfite modification of 5-methyldeoxycytidine and deoxycytidine residues. *Nucleic Acids Res.*, **8**, 4777–4790.
12. Herman,J.G., Graff,J.R., Myohanen,S., Nelkin,B.D. and Baylin,S.B. (1996) Methylation-specific PCR: a novel PCR assay for methylation status of CpG islands. *Proc. Natl Acad. Sci. USA*, **93**, 9821–9826.
13. Eads,C.A., Danenberg,K.D., Kawakami,K., Saltz,L.B., Blake,C., Shibata,D., Danenberg,P.V. and Laird,P.W. (2000) MethyLight: a high-throughput assay to measure DNA methylation. *Nucleic Acids Res.*, **28**, E32.
14. Cottrell,S.E., Distler,J., Goodman,N.S., Mooney,S.H., Kluth,A., Olek,A., Schwope,I., Tetzner,R., Ziebarth,H. and Berlin,K. (2004) A real-time PCR assay for DNA-methylation using methylation-specific blockers. *Nucleic Acids Res.*, **32**, e10.
15. Thomassin,H., Kress,C. and Grange,T. (2004) MethylQuant: a sensitive method for quantifying methylation of specific cytosines within the genome. *Nucleic Acids Res.*, **32**, e168.
16. Singer,J., Roberts-Ems,J. and Riggs,A.D. (1979) Methylation of mouse liver DNA studied by means of the restriction enzymes msp I and hpa II. *Science*, **203**, 1019–1021.
17. Bird,A.P. and Southern,E.M. (1978) Use of restriction enzymes to study eukaryotic DNA methylation: I. The methylation pattern in ribosomal DNA from *Xenopus laevis*. *J. Mol. Biol.*, **118**, 27–47.
18. Pollack,Y., Stein,R., Razin,A. and Cedar,H. (1980) Methylation of foreign DNA sequences in eukaryotic cells. *Proc. Natl Acad. Sci. USA*, **77**, 6463–6467.
19. Feinberg,A.P. and Vogelstein,B. (1983) Hypomethylation distinguishes genes of some human cancers from their normal counterparts. *Nature*, **301**, 89–92.
20. Singer-Sam,J., Grant,M., LeBon,J.M., Okuyama,K., Chapman,V., Monk,M. and Riggs,A.D. (1990) Use of a HpaII-polymerase chain reaction assay to study DNA methylation in the Pgk-1 CpG island of mouse embryos at the time of X-chromosome inactivation. *Mol. Cell. Biol.*, **10**, 4987–4989.
21. Singer-Sam,J., LeBon,J.M., Tanguay,R.L. and Riggs,A.D. (1990) A quantitative HpaII-PCR assay to measure methylation of DNA from a small number of cells. *Nucleic Acids Res.*, **18**, 687.
22. Bastian,P.J., Palapattu,G.S., Lin,X., Yegnasubramanian,S., Mangold,L.A., Trock,B., Eisenberger,M.A., Partin,A.W. and Nelson,W.G. (2005) Preoperative serum DNA GSTP1 CpG island hypermethylation and the risk of early prostate-specific antigen recurrence following radical prostatectomy. *Clin. Cancer Res.*, **11**, 4037–4043.
23. Cross,S.H., Charlton,J.A., Nan,X. and Bird,A.P. (1994) Purification of CpG islands using a methylated DNA binding column. *Nature Genet.*, **6**, 236–244.
24. Brock,G.J., Huang,T.H., Chen,C.M. and Johnson,K.J. (2001) A novel technique for the identification of CpG islands exhibiting altered methylation patterns (ICEAMP). *Nucleic Acids Res.*, **29**, E123.
25. Shiraishi,M., Chuu,Y.H. and Sekiya,T. (1999) Isolation of DNA fragments associated with methylated CpG islands in human adenocarcinomas of the lung using a methylated DNA binding column and denaturing gradient gel electrophoresis. *Proc. Natl Acad. Sci. USA*, **96**, 2913–2918.
26. Rauch,T. and Pfeifer,G.P. (2005) Methylated-CpG island recovery assay: a new technique for the rapid detection of methylated-CpG islands in cancer. *Lab. Invest.*, **85**, 1172–1180.
27. Ballestar,E., Paz,M.F., Valle,L., Wei,S., Fraga,M.F., Espada,J., Cigudosa,J.C., Huang,T.H. and Esteller,M. (2003) Methyl-CpG binding proteins identify novel sites of epigenetic inactivation in human cancer. *EMBO J.*, **22**, 6335–6345.

28. Bakker,J., Lin,X. and Nelson,W.G. (2002) Methyl-CpG binding domain protein 2 represses transcription from hypermethylated pi-class glutathione S-transferase gene promoters in hepatocellular carcinoma cells. *J. Biol. Chem.*, **277**, 22573–22580.

29. Lin,X. and Nelson,W.G. (2003) Methyl-CpG-binding domain protein-2 mediates transcriptional repression associated with hypermethylated GSTP1 CpG islands in MCF-7 breast cancer cells. *Cancer Res.*, **63**, 498–504.

30. Wade,P.A. (2001) Methyl CpG-binding proteins and transcriptional repression. *Bioessays*, **23**, 1131–1137.

31. Feng,Q. and Zhang,Y. (2001) The MeCP1 complex represses transcription through preferential binding, remodeling, and deacetylating methylated nucleosomes. *Genes Dev.*, **15**, 827–832.

32. Weber,M., Davies,J.J., Wittig,D., Oakeley,E.J., Haase,M., Lam,W.L. and Schubeler,D. (2005) Chromosome-wide and promoter-specific analyses identify sites of differential DNA methylation in normal and transformed human cells. *Nature Genet.*, **37**, 853–862.

33. Yegnasubramanian,S., Kowalski,J., Gonzalgo,M.L., Zahurak,M., Piantadosi,S., Walsh,P.C., Bova,G.S., De Marzo,A.M., Isaacs,W.B. and Nelson,W.G. (2004) Hypermethylation of CpG islands in primary and metastatic human prostate cancer. *Cancer Res.*, **64**, 1975–1986.

34. Nakayama,M., Bennett,C.J., Hicks,J.L., Epstein,J.I., Platz,E.A., Nelson,W.G. and De Marzo,A.M. (2003) Hypermethylation of the human glutathione S-transferase-pi gene (GSTP1) CpG island is present in a subset of proliferative inflammatory atrophy lesions but not in normal or hyperplastic epithelium of the prostate: a detailed study using laser-capture microdissection. *Am. J. Pathol.*, **163**, 923–933.

35. Lee,B.H., Yegnasubramanian,S., Lin,X. and Nelson,W.G. (2005) Procainamide is a specific inhibitor of DNA methyltransferase 1. *J. Biol. Chem.*, **280**, 40749–40756.

36. Clark,S.J., Harrison,J., Paul,C.L. and Frommer,M. (1994) High sensitivity mapping of methylated cytosines. *Nucleic Acids Res.*, **22**, 2990–2997.

37. Fraga,M.F., Ballestar,E., Montoya,G., Taysavang,P., Wade,P.A. and Esteller,M. (2003) The affinity of different MBD proteins for a specific methylated locus depends on their intrinsic binding properties. *Nucleic Acids Res.*, **31**, 1765–1774.

38. Klose,R.J., Sarraf,S.A., Schmiedeberg,L., McDermott,S.M., Stancheva,I. and Bird,A.P. (2005) DNA binding selectivity of MeCP2 due to a requirement for A/T sequences adjacent to methyl-CpG. *Mol. Cell*, **19**, 667–678.

39. Hu,M., Yao,J., Cai,L., Bachman,K.E., van den Brule,F., Velculescu,V. and Polyak,K. (2005) Distinct epigenetic changes in the stromal cells of breast cancers. *Nature Genet.*, **37**, 899–905.

40. Lippman,Z., Gendrel,A.V., Black,M., Vaughn,M.W., Dedhia,N., McCombie,W.R., Lavine,K., Mittal,V., May,B., Kasschau,K.D. *et al.* (2004) Role of transposable elements in heterochromatin and epigenetic control. *Nature*, **430**, 471–476.

41. Lippman,Z., Gendrel,A.V., Colot,V. and Martienssen,R. (2005) Profiling DNA methylation patterns using genomic tiling microarrays. *Nature Methods*, **2**, 219–224.

42. Song,F., Smith,J.F., Kimura,M.T., Morrow,A.D., Matsuyama,T., Nagase,H. and Held,W.A. (2005) Association of tissue-specific differentially methylated regions (TDMs) with differential gene expression. *Proc. Natl Acad. Sci. USA*, **102**, 3336–3341.